Spinodal decomposition in AISI 316L stainless steel via high-speedlaser remelting

Evans Chikarakara[a] , Sumsun Naher[b], Dermot Brabazon[a]
[a]Advanced Processing Technology Research Centre, Dublin City University, Dublin, Ireland
[b]School of Engineering and Mathematical Sciences, City University London, UK

Keywords: Laser remelting, Spinodal decomposition, Lamellar and nodular structures316L, stainless steel

ABSTRACT

A 1.5 kW CO_2 pulsed laser was used to melt the surface of AISI 316L stainless steel with a view to enhancing the surface properties for engineering applications. A 90 m laser beam spot size focused onto the surface was used to provide high irradiances (up to 23.56MW/cm^2) with low residence times (as low as 50 μs) in order to induce rapid surface melting and solidification. Variations in microstructure at different points within the laser treated region were investigated. From this processing refined lamellar and nodular microstructures were produced. These sets of unique microstructures were produced within the remelted region when the highest energy densities were selected in conjunction with the lowest residence times. The transformation from the typical austenitic structure to much finer unique lamellar and nodular structures was attributed to the high thermal gradients achieved using these selected laser processing parameters. These structures resulted in unique characteristics including elimination of cracks and a reduction of inclusions within the treated region. Grain structure reorientation between the bulk alloy and laser-treated region occurred due to the induced thermal gradients. This present article reports on microstructure forms resulting from the high-speed laser surface remelting and corresponding underlying kinetics.

1. Introduction

Austenitic stainless steel is used in wide range of applications that require high corrosion resistance, ductility, strength, formability, and weldability. 316L stainless steel in particular is extensively used in biomedical implants, nuclear core internal structures and piping applications due to its excellent corrosion resistance properties [1,2]. It should be noted though that 316L steel may corrode under certain circumstances in a highly stressed and oxygen depleted environment. Therefore an impetus still exists to further modify the surface of the metal to improve its wear resistance, corrosion resistance and fatigue strength [2].

Mechanical properties of 316L stainless steel are a function of its microstructures, and consequently, its thermal history [3]. Heat treatment at low cooling rates does not provide significant material property benefits. Studies have shown that stainless steel subjected to a low temperature spinodal decomposition in which the ferrite decomposes into an iron-rich and a chromium-enriched results in embrittlement, due to hardening of the ferrite phase [4,5]. Laser melting on the other hand can produce extremely high cooling rates, up to 10^6 K/s, which prevents common low temperature phase transformations from occurring due to the limited time provided in which the reaction is thermodynamically favourable and

kinetically accessible. This can allow for reduced crystallinity thereby increasing the mechanical properties such as hardness and wear resistance.

Carbon in iron alloys significantly influences the mechanical properties of ferrite even with a small weight percentage (e.g. 0.2%). In steel microstructures, fine pearlitic structure and small grain sizes typically provide optimal conditions for laser processing [6–8]. If the structure was made up of coarse graphite with large grains it would not respond as well to laser hardening, preventing the complete transformation from the austenitic phase to the martensitic phase. The final hardness of the steel is directly related to the quantity of residual austenite or martensite formed during laser hardening. Steel alloys can be heat treated down to greater depths than plain carbon steel due to their lower thermal conductivity. Research to date suggests that laser treating could be a preferred method at inducing the formation of retained martensite due to the extremely low quenching times [9].

Steels that can be heat-treated are typically of high carbon con-tent [10]. AISI 316L stainless steel is extremely difficult to heat-treatfor hardness due to its low carbon content. Carbon enrichment andsurface alloying methods are therefore sometimes implemented before heat treatment operations, in order to successfully heat treat 316L stainless steel [11].

Such treatments induce high hardness, improved wear resistance and reduced cracks throughout the sample, however they tend to be complex and produce nonhomogeneous results. The current study focuses on high-speed laser remelting which is a low cost, low complexity and highly repeatable surface treatment due to elimination of the requirement of material addition. High-speed laser remelting is known to produce a refined microstructure capable of significantly improved hardness, wear and corrosion resistance [12]. This article presents fundamental aspects and mechanisms of the formation of these structures within 316L.

2. Experimental

Cylindrical AISI 316L austenitic stainless steel samples 120 mm long and 10 mm in diameter were laser melted using a, 1.5 kW Rofin DC015 slab CO_2 laser (10.6 m wavelength). The composition of the as-received material is given in Table 1.

A Gaussian beam spot size of 90 m was utilised for all treatments. Experiments were carried out by varying irradiance (calculated from the peak power) and residence time ranging from 7.86 to 23.58MW/cm^2 and from 50 to 167s, respectively. The combination of these parameters provided a fluence range from 393 to 3930J/cm2. This present work focused on samples treated at the high irradiance and low residence time; specifically, samples treated at fluences of 950 and 2096J/cm^2 with each sample repeated three times. A detailed study of the effects of processing parameters on melt pool depth and surface roughness is presented elsewhere [13].

Table 1
Elemental chemical composition of AISI 316L stainless steel (weight %).

Element	Cr	Ni	Mo	Mn	Si	Co	N	S	P	C	Fe
wt.%	16.82	10.14	2.03	1.51	0.55	0.08	0.061	0.03	0.03	0.02	Bal.

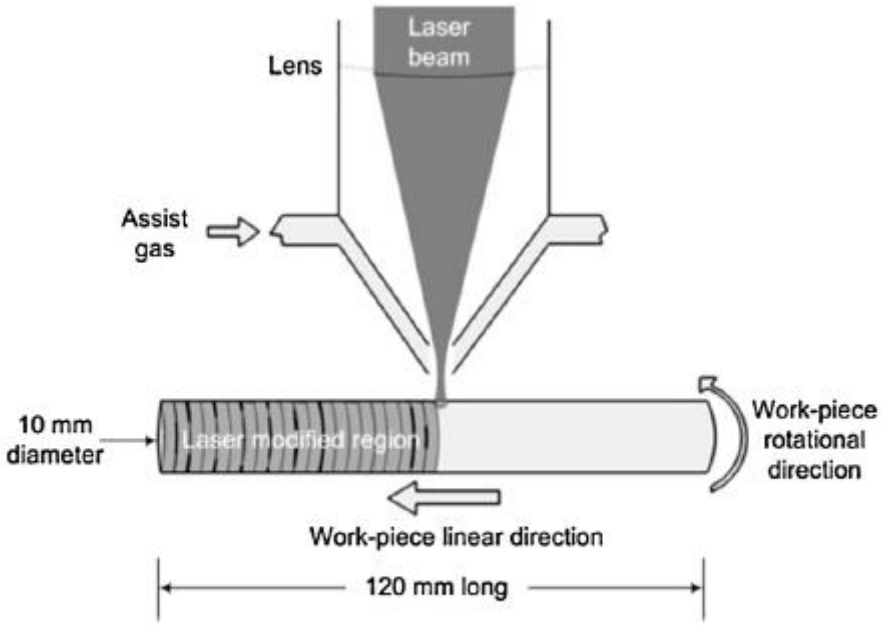

Fig. 1. Schematic of the laser processing set-up for a cylindrical sample.

Argon was used as an assist gas to shield the melt pool thus avoiding oxidation during laser processing. In order to achieve very low residence times, high sample speeds had to be implemented. Previous studies have shown that extreme temperature gradients can be attained by using rotating cylindrical samples at high speeds [10]. The samples were rotated using a DC motor, attached to the sample positioning stage, capable of speeds of up to 2500 rpm. Fig. 1 illustrates the laser processing set-up.

In order to visualise grain boundaries and phases within the samples, they were chemically etched using Glyceregia. The influence of the process parameters on the microstructure of the modified surface topology and cross section were studied using the scanning electron microscopy (SEM). Microstructure details investigated included pits and cracks, grain structure and sizes, interfacial-voids and inclusions.

3. Results

Fig. 2 shows SEM images of (a) planar and (b) cross-sectional microstructure prior to laser surface modification. The as-received surface (Fig. 2a) shows an uneven topology with significantly large scratches and cracks.

The cross-sectional micrographs (Fig. 2b) show the phases present in 316L stainless steel. Small pores are visible as dark spots on the BSE micrographs. These are likely to be caused by the pull out of inclusions in the steel during grinding and polishing. Fig. 3(a) shows the SEM image of the steel laser remelted at an energy density range of 950J/cm^2. The cross-sectional micrographs (Fig. 3b) show the grain structure and phases present within the laser treated 316L stainless steel.

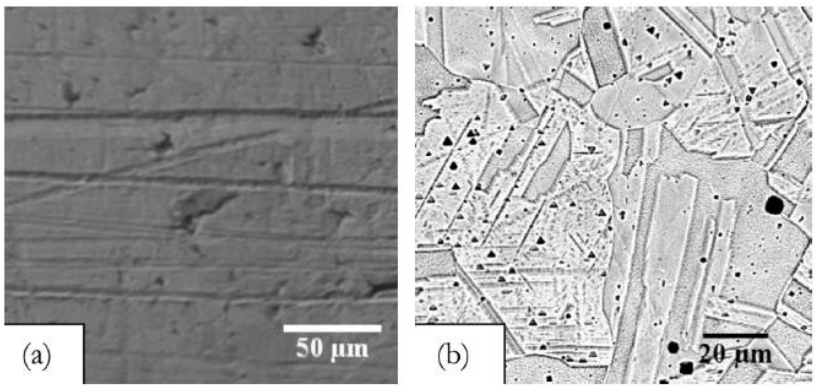

Fig. 2. Microstructure of as-received 316L stainless steel (a) morphology structure and (b) the cross-sectional microstructure obtained via secondary electron (SE) detector.

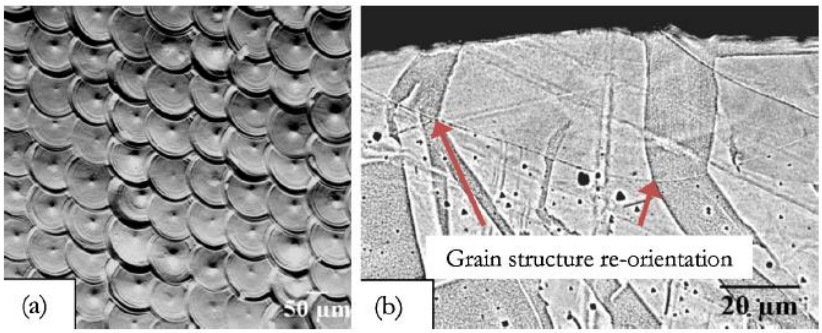

Fig. 3. Microstructure 316L stainless steel (a) topological view of surface morphology after laser treatment at 950 J/cm^2 and (b) cross-sectional view of a laser sample treated at 950 J/cm^2.

Laser surface melting observed was a typical melting morphology with no voids, inclusions, pits or cracks. A prominent feature observed on the cross-section was grain structure re-orientation at the bulk alloy-treated interface. The phenomenon was visible in all samples treated at energy densities greater than 900J/cm^2.

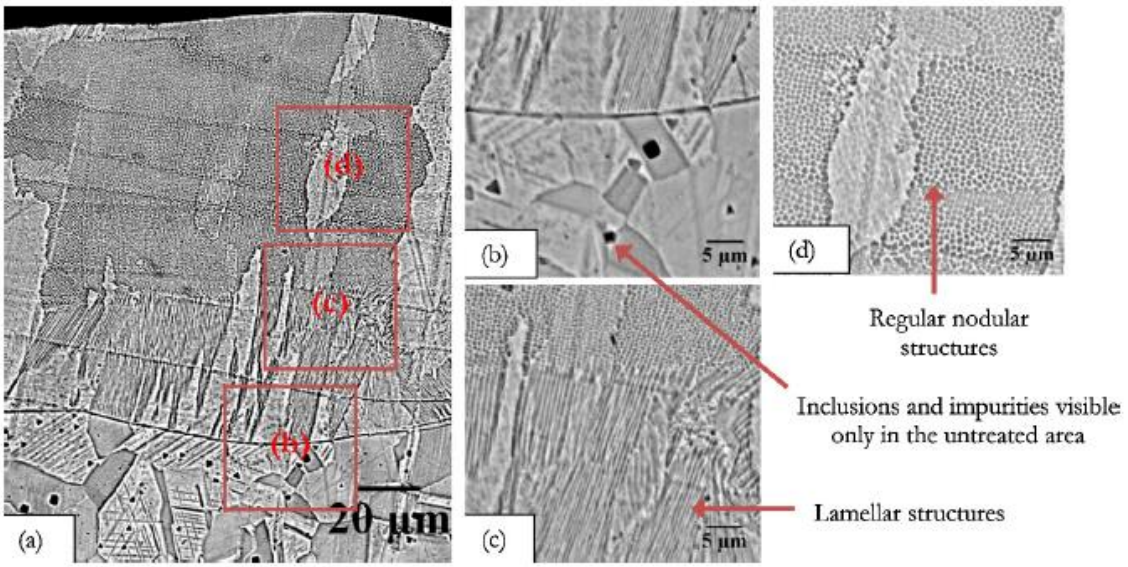

Fig. 4. (a) Microstructure variation in samples treated at 2096 J/cm^2 and magnified view of specific regions (b), (c) and (d).

Fig. 4(a) depicts the surface and cross-sectional microstructure produced at a high energy density of 2096J/cm^2. An increase in depth of processing was observed as a result of processing at higher energy density. Grain size and orientation alteration is visible from Fig. 2. The overlapping boundaries visible at high energy density of 2096J/cm^2 can be seen in Fig. 4(a) as layers representing different isotherms. Fig. 4(b) is a magnified view, of Fig. 4(a), showing the interface between the untreated and laser surface modified (LSM) regions, highlighting grain structure re-orientation and transition of the grain structure from the typical austenite grain structure into a lamellar structure. Fig. 4(c) shows the transition from lamellar structures to nodular structures. The nodular structure, shown in Fig. 4(d), is prevalent near the surface. This structure has not previously been identified in literature. The aforementioned microstructures were observed in all samples treated at that specific energy density signifying a degree of repeatability. It is postulated that the transition is caused by the high cooling rates and thermal gradient induced by the combination of high irradiance and low residence times. In addition, no cracks were visible on the laser treated region subsequent to processing at 2096 J/cm^2.

4. Discussion

Processing parameters used in this study were carefully chosen so that energy densities would not exceed levels that induce ablation of the surface material. From the previous studies, it was established that energy densities greater than 6700J/cm^2 resulted in ablation regardless of the residence time [13]. At this energy level sample sparking was observed. The grain direction re-orientation is attributed to the tangential forces, produced from the rotation of the sample, on the laser melted material. Even though the residence time was very low, the cooling rates were still not high enough to significantly impact the grain sizes. There was no significant grain size changes observed in the sample laser treated at 950J/cm^2.

Roughness and ripple-like features visible on the surface of the treated zone in addition to the cross sectional observed melt pool regions evidenced that the material reached liquid phase. When the surface was laser melted a dimpled region was formed from the resolidified material [10]. The set overlap was set to 30%, however was measured on the processed sampled to be between 20% and 25%. This phenomenon can be attributed to the Gaussian nature of the TEM_{00} laser beam. The beam intensity drops from the centre towards the outer edge in the shape of a normal distribution[14]. The effective diameter of such a laser beam is quantified as the distance at which the irradiance is $1/e^2$ of the maximum peak irradiance. In this case, only 86.5% of the total laser beam power lies within this region since 1/e2. The remainder of this energy outside this point is regarded as insufficient to impact the material thus resulting in the reduced overlap percentage. The lamellar morphology created at this interface in the LSM region resembles the grain structure after diffusionless transformation as presented in the ASM Handbook Vol. 9 [15]. These martensitic-like structures are produced by rapid quenching of the austenitic parent phase.

The austenitic phase is not retained due to the uninterrupted rapid cooling which prevents austenitic decomposition into ferrite and pearlite via diffusional processes. The substrate acts as a heat sink thus assisting with achieving the rapid solidification necessary for formation of this structure. The novel nodular microstructure in 316L stainless steel is highly likely due to sequence of events which initiate when the laser beam contacts the surface. Firstly, the near

surface region rapidly reaches the melting point and then a liquid/solid interface starts to move initially away from the surface to the determined melt pool depth. At this stage the maximum melt depth has been attained, interatomic diffusion continues, and the liquid/solid interface velocity is momentarily zero. The interface then rapidly moves back to the surface with inter-atomic diffusion continuing in the liquid. However, the re-solidified metal behind the liquid/solid interface cools so rapidly that solid state diffusion is negligible compared to that expected from an equilibrium phase diagram. Finally, resolidification is completed and a surface modified layer has been created. Due to the relatively small depth of the melted zone (10–100 m), very high quench rates are achieved resulting in nonequilibrium microstructure formation [16].

5. Conclusions

The paper presented effects of high-speed laser surface modification on the resultant microstructure of 316L stainless steel. The sequences following laser beam interaction and surface melting resulted in the formation of the unique lamellar and nodular structures in 316L stainless steel. The processing parameters used in this research produced extremely high cooling rates and high thermal gradients capable of eliminating asperities, cracks and inclusions within the treated region. The formation of the unique nodular structures was attributed to high temperature and cooling rate spinodal decomposition. The high degree of repeatability, homogeneity of treatment and localised nature of the treatment suggest that laser remelting could be a possible replacement of laser alloying and cladding in surface property enhancement applications. Further analysis of resultant hardness, as well as wear and corrosion resistance is needed to more fully evaluate the potential benefits of these surfaces. The current study has highlighted unique microstructural modifications that can be achieved with 316L via a low cost, low complexity and highly repeatable high-speed laser remelting surface treatment.

Acknowledgement

The authors sincerely thank the Office of Vice President of Research (OVPR), Dublin City University, for the financial support for this work.

References

[1] A.J. Sedriks, Corrosion of Stainless Steels, Electrochemical Society, Wiley, 1979.

[2] J.D. Bronzino, The Biomedical Engineering Handbook, 2nd ed., CRC Press, Boca Raton, FL, 2000.

[3] W.D. Callister, Materials Science and Engineering: An Introduction, Wiley, New York, 2000.

[4] K. Chandra, V. Kain, V. Bhutani, V.S. Raja, R. Tewari, G.K. Dey, Low temperature thermal aging of austenitic stainless steel welds: kinetics and effects on mechanical properties, Mater. Sci. Eng. A 534 (2012) 163–175.

[5] S.S. Brenner, M.K. Miller, W.A. Soffa, Spinodal decomposition of iron-32 at.% chromium at 470◦C, Scripta Metall. Mater. 16 (1982) 831–836.

[6] M. Pellizzari, M.G. De Flora, Influence of laser hardening on the tribological properties of forged steel for hot rolls, Wear 271 (2011) 2402–2411.

[7] A. Lasalmonie, J.L. Strudel, Influence of grain size on the mechanical behaviour of some high strength materials, J. Mat. Sci. 21 (1986) 1837–1852.

[8] J. Hyzak, I. Bernstein, The role of microstructure on the strength and toughness of fully pearlitic steels, Metall. Mat. Trans. A. 7 (1976) 1217–1224.

[9] J.C. Ion, Laser transformation hardening, Surf. Eng. 18 (2002) 14–31.

[10] J.F. Ready, D. Farson, LIA Handbook of Laser Materials Processing, Laser Institute of America, Orlando, 2001.

[11] F. Laroudie, C. Tassin, M. Pons, Laser surface alloying of 316L stainless steel: different hardening routes and related microstructures, J. Phys. IV 4 (1994) 77–80.

[12] E. Chikarakara, S. Naher, D. Brabazon, High speed laser surface modification of Ti-6Al-4V, Surf. Coat. Technol. 206 (2012) 3223–3229.

[13] E. Chikarakara, S. Naher, D. Brabazon, Process mapping of laser surface modification of AISI 316L stainless steel for biomedical applications, Appl. Phys. A 101 (2011) 367–371.

[14] Y.A. Alsultanny, Laser beam analysis using image processing, J. Comp. Sci. 2 (2006) 109–113.

[15] G.R. Speich, Martensitic structures, in: G.F. Vander Voort (Ed.), ASM Handbook, Metallography and Microstructures, vol. 9, ASM International, Ohio, 2001.

[16] T.N. Baker, Laser surface modification of Ti alloys, in: H. Dong (Ed.), Surface Engineering of Light Alloys: Aluminium, Magnesium and Titanium Alloys, Woodhead Publishing Ltd., Cambridge, UK, 2009.